Published in final edited form as:
*Curr Mol Med*. 2013 December ; 13(10): 1523–1537.

# Antibody-Based Imaging of HER-2: Moving into the Clinic

**Rongsheng E. Wang**[1,*], **Yin Zhang**[2], **Ling Tian**[1], **Weibo Cai**[2], and **Jianfeng Cai**[3]
[1]Mediomics, LLC, St Louis, MO, USA

[2]Departments of Radiology and Medical Physics, University of Wisconsin-Madison, WI, USA

[3]Department of Chemistry, University of South Florida, Tampa, FL, USA

## Abstract

Human epidermal growth factor receptor-2 (HER-2) mediates a number of important cellular activities, and is up-regulated in a diverse set of cancer cell lines, especially breast cancer. Accordingly, HER-2 has been regarded as a common drug target in cancer therapy. Antibodies can serve as ideal candidates for targeted tumor imaging and drug delivery, due to their inherent affinity and specificity. Advanced by the development of a wide variety of imaging techniques, antibody-based imaging of HER-2 can allow for early detection and localization of tumors, as well as monitoring of drug delivery and tissue's response to drug treatment. In this review article, antibody-based imaging of HER-2 are summarized and discussed, with an emphasis on the involved imaging methods.

### Keywords

Antibody; Drug delivery; Radioimmunoscintigraphy (RIS); Positron emission tomography (PET); Single-photon emission computed tomography (SPECT); Magnetic resonance imaging (MRI); Near-infrared fluorescence (NIRF) imaging; Photoacoustic tomography (PAT)

## INTRODUCTION

The epidermal growth factor (EGF) and EGF receptor (EGFR) are one of the first discovered pairs of growth factor ligand-receptor, with EGFR later recognized as a member of a receptor tyrosine kinase family, the human epidermal growth factor receptor (HER) family [1]. The HER family comprises four structurally related members: EGFR (HER-1 or erythroblastic leukemia viral oncogene homolog 1 [ErbB1]), HER-2 (ErbB2), HER-3 (ErbB3), and HER-4 (ErbB4) [2, 3]. The structure of every HER family member consists of an N-terminal extracellular domain (ECD), a single membrane-spanning region and a C-terminal cytoplasmic domain, among which the ECD acts as a receptor to bind with ligands [1, 4]. To date, a number of these ligands have been reported, such as EGF, β-cellulin, amphiregulin, and transforming growth factor-alpha (TNF-α) [2, 3]. Upon binding, the ligand induces the dimerization of a HER-kinase that either homodimerizes with itself, or heterodimerizes with other HER family members [1]. As a result of the dimerization, the HER-kinases undergo conformational changes, which promote the activation of the cytoplasmic domain with a subsequent phosphorylation leading to various downstream signaling pathways and cellular events [1].

For Reprints please contact: Rongsheng E. Wang, Mediomics LLC, 5445 Highland Park Drive, St. Louis, MO, USA, rongshengwang@wustl.edu; Phone: 314-341-0544.

Among the HER family, one key member, HER-2, behaves in a unique way since it has no identified natural ligand yet. HER-2 is thereby activated only through its heterodimerization with other HER family members that have been pre-activated by their own ligands. For other HER family members, HER-2 is actually the preferred partner to form heterodimers, and the HER-2 involved heterodimerization is the most potent signal transduction pathway among all dimerizations of the HER family [5]. Hence, by mediating complex signaling pathways, HER-2 plays pivotal roles in cell growth, migration, differentiation and survival [4, 6–8]. From a genetic perspective, the HER-2 gene was derived from a potent oncogenic mutant in neuroglioblastomas developed in carcinogen exposed rats, and was originally termed NEU [9–11]. The gene amplification and protein over-expression of HER-2 can increase and prolong signals that trigger the transformation of cells, leading to tumorigenesis and metastasis [4]. The up-regulation of HER-2 is thereby commonly observed in human cancers, such as breast, ovarian, gastric, and prostate cancer [4, 12–14]. To date, both HER-2 and its involved signaling pathways have been extensively investigated as targets in cancer therapy, during which a direct inhibition of these proteins/pathways can block tumor proliferation. Moreover, the ECD of HER-2 is regarded as an ideal target for tumor-directed drug delivery [4].

One major strategy for HER-2 targeting is to use monoclonal antibodies (mAbs), among which trastuzumab was the first Food and Drug Administration (FDA) approved anti-HER-2 antibody [11, 15]. Trastuzumab, also known as Herceptin, binds to the ECD of HER-2 and induces apoptosis in HER-2 over-expressing cancer cells [4, 11]. Another humanized anti-HER-2 mAb is pertuzumab, which binds to a different subdomain of HER-2's ECD and thereby sterically inhibits the dimerization of HER-2 with itself and other HER family members [16]. Clinically, pertuzumab displayed promising therapeutic activities and tolerable toxicities [17]. A synergy of trastuzumab and pertuzumab also resulted in an enhanced antitumor effect *in vivo* [18, 19]. Besides antibodies, another strategy is to use tyrosine kinase inhibitors to target the intracellular domain of HER-2, among which lapatinib has been well characterized, and is currently in clinical trials [20]. Alternatively, some other protein inhibitors [21, 22], as well as agents to knock out HER-2 mRNA [23, 24], have also been reported.

Whereas an intensive attention has been paid to HER-2 targeted therapy, increasing interests also arise in HER-2 based molecular imaging. The effectiveness of HER-2 targeted therapy highly depends on accurate evaluation of its expression level in tumors. It is recommended by the American Society of Clinical Oncology (ASCO) to characterize HER-2 levels on primary breast cancer at the time of either diagnosis or recurrence [25]. By using contrast agents or probes, noninvasive molecular imaging techniques allow for direct visualization of the targeting process including bio-distribution and pharmacokinetics, as well as spatiotemporal monitoring of cellular activities/responses in the targeted region. As mentioned above, antibodies against HER-2 are the mainstream of the developed therapeutics for treating HER-2 over-expressing cancer. For HER-2 detection and imaging, they are also the most commonly used agents [11]. Antibody-based imaging not only renders more insights into the HER-2 targeting process, but also identifies and localizes the HER-2 expressing tumors, which facilitates the subsequent drug delivery and the follow-up evaluation of therapeutic results. Herein, we systematically summarize and discuss the applications of antibodies for diagnostic imaging of HER-2, using a variety of imaging techniques. Several practical examples including clinical applications are also highlighted for each imaging approach.

## ANTIBODIES AS TARGETING AGENTS

Antibodies, also known as immunoglobulins, have become desirable molecules for use as research tools, diagnostic agents, and therapeutic drugs. There are five isotypes of human antibodies (i.e. IgA, IgD, IgE, IgG, and IgM), among which IgG is the most abundant and versatile type that constitutes 75 percent of serum immunoglobulins [26, 27]. IgG is a Y-shaped, multi-domain protein composed of two Fab arms and one Fc stem [28]. The antigen-binding sites are located on the tips of the Fab arms, while the Fc domain recruits effector functions and maintains long serum half-lives of the antibody, by interacting with a diverse set of receptors [29]. The introduction of the hybridoma technology by Kohlerand Milstein in 1975 [30] set the starting point of the antibody industry. Subsequently, other technical invention to generate humanized monoclonal antibody (mAb) and chimeric mAb further resolved the issues in immunogenicity and low efficacy [31, 32]. In many applications of antibodies such as imaging, the Fc-mediated effects are not necessary and may even compromise certain function/properties of the antibody [29]. Advanced by recombinant DNA technology and protein engineering, the Fc domain and associated effects can be removed to render monovalent and bivalent mAb fragments and engineered variants, such as Fab, F(ab′), single chain Fv (scFv), minibodies, diabodies, affibodies, nanobodies and anticalins [28, 33–35]. Among these engineered fragments, affibody is the most commonly used in imaging, which is a small 58-amino acid Z-domain scaffold derived from the IgG-binding domain of *staphylococcal* protein A [36]. The binding surface of affibody has a randomized sequence of 13 amino acids, which can be screened to generate a specific sequence recognizing the desired target [34, 37]. For HER-2 targeting, the affibody molecule $His_6$-$Z_{HER\text{-}2/neu:4}$ was shown to bind the ECD of HER-2 with nanomolar affinity [38].

To date, development of antibodies for diagnostic and therapeutic applications has become the fastest growing area in biopharmaceutical research, with over 100 mAbs currently in clinical trials [31] and more than 20 already approved for clinical use [39]. Besides being therapeutic agents, antibodies also play pivotal roles as targeting ligands to direct the delivery of chemotherapeutics and imaging contrast agents to the tissue of interest. Compared to traditional drugs, antibody-drug conjugates (ADCs) control the bio-distribution of the drugs that are cytotoxic in most cases, thereby sparing their contacts from normal tissues and providing a high intratumoral drug concentration [40]. Antibody specificity is crucial to the success of antibody directed drug delivery, where the targeted antigen should be substantially up-regulated on tumor cells but not on normal tissue cells [40]. This specificity allows the use of highly potent drugs that would otherwise be too toxic for healthy cells. Additionally, the stability of the linker (which ensures drug release only after targeting) and the conjugation method (which affects the drug loading stoichiometry and homogeneity) are both important factors to be considered [40]. Currently, there are three common methods for conjugation of mAbs: alkylation of reduced inter-chain disulfides, alkylation of genetically engineered cysteine, and acylation of lysine, among which the cysteine conjugation provides a greater degree of uniformity by allowing site-specific introduction of cysteines into the mAb and subsequent attachment of drugs at the defined stoichiometry [41–43].

There are several challenges in antibody-based imaging of HER-2. An efficacious delivery and high contrast imaging is often accompanied by antibodies' high avidity to the target and their relatively long retention time in the target region. In reality, however, a large fraction of antibodies rapidly detach from their binding sites, especially under the high shear stress of physiological relevance. To generate antibodies with the desired high affinity, phage display technique was adopted for customized engineering of humanized antibodies [44]. Another issue besides the affinity is the formidable barriers imposed by solid tumors to resist the

penetration of drugs or delivery agents, which largely diminishes the values of *in vitro* experiments [45]. It was also shown that once nanoparticles or microbubbles were conjugated to antibodies, the combined sizes of the resulting conjugates could slow down the delivery speed [45]. Despite these drawbacks, antibody-based imaging of HER-2 represents one of the most promising strategies for clinical management of breast cancer, which has recently attracted intensive research interests.

## RADIOIMMUNOSCINTIGRAPHY (RIS)

Radiolabeling of antibodies was initially used to circumvent several problems encountered in the therapeutic development of antibody conjugated chemotherapeutics or toxins. To be efficacious, it is required that every malignant cell expresses the target antigen, which is usually not the case in practice [27]. However, drugs may be susceptible to degradation in endocytosis during drug delivery, and toxins can easily induce immunogenicity. Furthermore, a variable percentage of tumor cells can develop multidrug resistance. Compared to these traditional approaches, radioisotopes bear certain advantages in which tumor cells cannot develop resistance against irradiation and the particles emitted by radionuclides can kill adjacent tumor cells [27]. Whereas the volume of drugs to be conjugated may affect the antibodies' transportation and delivery, an alternative conjugation with small sized radioisotope can achieve a high specificity with about 20: 1 tumor-to-normal-tissue ratio [27]. Therefore, radioimmunotheraphy (RIT) has become a common approach to complement surgery and chemotherapy, although its efficacy is still limited in certain cancer types such as medullary thyroid carcinoma (MTC) [29].

Another application of isotopes is radioimmunoscintigraphy (RIS), which can determine the extent of disease, monitor the effect of therapy, and detect tumor recurrence [46]. In a typical procedure, a radiolabeled antibody is injected into patients intravenously, and the gamma ray emission from the radiolabeled antibody can be captured by gamma cameras to generate two-dimensional images. RIS detects antigens at a cellular level and has certain advantages in sensitivity over other existing imaging techniques, such as magnetic resonance imaging (MRI), computerized tomography (CT), and ultrasound (US) [46, 47], which primarily detect general morphological changes and are thereby fundamentally different from RIS in the underlying mechanism [48]. RIS is also different from other imaging techniques such as positron emission tomography (PET), single-photon emission computed tomography (SPECT), and X-ray. In the case of diagnostic X-ray, an external radiation was employed to pass through the body for image acquisition. For PET and SPECT, they generate three-dimensional images.

The common radionuclides used in RIT and RIS are $^{67}$Cu, $^{177}$Lu, $^{186}$Re, $^{188}$Re, $^{125}$I, $^{111}$In, and $^{99m}$Tc [27, 49]. In a pilot study in mouse xenograft models, $^{125}$I-labeled 741F8-2 (scFv′)$_2$ homodimer displayed higher specificity to human SKOV-3 tumors than other antibody fragments, resulting in an enhanced tumor contrast in sagittal section autoradiography [50]. Subsequently, trastuzumab Fab was radiolabeled with $^{111}$In, which specifically localized HER-2-positive BT-474 human breast cancer xenograft in athymic mice [51]. Around 24 hours after administration of the radiolabeled antibody, tumors as small as 3 ~ 5 mm in diameter could be detected by imaging. A much improved HER-2 imaging has been achieved with affibodies, such as $^{125}$I-labeled $(Z_{HER-2:4})_2$ [52] , $^{111}$In-labeled $Z_{HER-2:342-pep2}$ [53] or ABY-025 [54], and $^{99m}$Tc-labeled $Z_{HER-2:342}$ [55] (Fig. (1)), which all afforded high-contrast gamma camera images. Following the success in animal models, $^{111}$In-labeled trastuzumab was administered to patients with HER-2 expressing breast cancer [56, 57]. Clinical imaging demonstrated an accurate detection of HER-2-positive tumors. It is noteworthy that this trastuzumab-based tracer did not induce undesired

immune response in the body, and exhibited a satisfactory biodistribution in tumors and normal organs.

## POSITRON EMISSION TOMOGRAPHY (PET)

PET has been widely used in medical diagnostics and biochemical research including oncology, neurology, and cardiology [58–63]. The radiolabeled agents, using positron emitters, are intravenously injected to the body, circulated, and collectively retained in tissues according to their biological properties [64]. The positron-electron annihilation generates a pair of 511 keV gamma photons in opposite directions, which can escape from the body and be detected and reconstructed to generate three-dimensional images. The signal intensity of every voxel is proportional to the amount of radioactive agents, thereby allowing PET to quantitatively map the spatial dispersion of radioactive agents all over the body. When serial PET images over a time course are collected, the time-dependent spatial distribution of radiotracers can be obtained, thereby allowing the monitoring and characterization of biological phenomena of interest [64].

Two common approaches are adopted for immunoPET imaging [65]. In the first approach, PET probes are constructed based on fast kinetic antibodies, which can be applied for fast imaging at low radiation levels, to confirm the target presence and scout the proper person for following-up therapies [65, 66]. Smaller antibody fragments (scFv, diabodies, minibodies, etc) are routinely used in this approach, which retain the binding specificity of the parent antibodies, but have different pharmacokinetic characteristics such as quicker clearance from the body, and relatively low tumor uptake [67]. In the second approach, radiolabeled antibodies are administered for imaging in a pre- or early course of therapies, to gain a sight of the targeting efficiency, the *in vivo* behavior of antibodies, as well as the therapeutic responses [65]. In this regard, intact antibodies are well suited materials in terms of their long residence in circulation (1–3 weeks), which allows for a specific and prominent accumulation of radiotracers in tumor cells, as well as long intervals between administrations [67]. For both approaches, the decay half-life of the used radionuclides should match the circulation half-life of the antibodies to be conjugated to. Hence, radioisotopes $^{11}$C, $^{68}$Ga, $^{18}$F, $^{64}$Cu, $^{86}$Y, and $^{76}$Br are commonly used for the first approach, while the long-lived positron emitters such as $^{89}$Zr or $^{124}$I are preferentially employed for the second approach [66–69].

In an early study, a minibody derived from trastuzumab was radiolabeled and shown by quantitative microPET to preferentially localize in the kidneys, thereby not ideal as an imaging agent [70]. By manipulating the size and format, a slightly larger antibody fragment, the 105 kDa scFv-Fc was designed and demonstrated to have an increased tumor uptake and a reduced kidney uptake. Compared to the whole antibody molecule, this scFv-Fc fragment was still tailored in structure to possess a fast clearance in blood and normal tissues [70]. Subsequently, several trastuzumab-based antibodies or affibodies were labeled with radioisotopes, especially those long-lived ones, for PET imaging of HER-2 expressing human tumor xenografts [71–74]. Among these reports, affibody targeting provided better imaging contrast than that of a radiolabeled intact antibody, due to its better radioactivity retention and tumor specificity [74]. It is also notable that with PET imaging of $^{89}$Zr-trastuzumab, HER-2 down-regulation can be monitored during the tumor treatment by a heat shock protein 90 (HSP90) inhibitor [75] in a mouse model. Hence, immunoPET imaging of HER-2 can monitor the therapeutic responses of HER-2 positive tumors [73] (Fig. (2A,B)).

Using other radiolabeled HER-2 targeting antibodies, one can independently measure the HER-2 levels affected by trastuzumab treatment. For example, the C6.5 diabody can selectively target ECD of HER-2, in a region that is distinct from that bound by trastuzumab

[76]. The $^{124}$I-labeled C6.5 diabody was thus shown to be specifically taken up by several HER-2-positive tumor cell lines, and was thereby employed to monitor HER-2 status and to evaluate the results of trastuzumab treatment [77, 78].

Clinically, $^{89}$Zr-trastuzumab was stable for up to seven days in human serum, and had a minimal dose of 100 μg for optimal PET imaging [79]. $^{89}$Zr-trastuzumab based PET images were demonstrated to result in an excellent spatial resolution and a good signal-to-noise ratio, with tumor uptake observed in HER-2-positive lesions such as metastatic liver, lung, bone and brain (Fig. (2C,D)) [80]. The radiotracer uptake can also be quantified via PET scanning [79, 80], which may help the definition of optimal dosage for patient-specific trastuzumab therapy regimens [81]. On the other hand, probes at low doses will be subjected to rapid hepatic clearance, presumably due to high levels of circulating HER-2 ECD in plasma [80].

## SINGLE-PHOTON EMISSION COMPUTED TOMOGRAPHY (SPECT)

SPECT differs from PET in the method used to define the angle of incidence, in which the gamma rays are emitted as single photons and only those in the prescribed direction can be received by the detector [82, 83]. A variety of radioisotopes such as $^{99m}$Tc, $^{125}$I, and $^{131}$I can be used for SPECT [82, 84–88], which does not require complicated facilities such as cyclotron for PET imaging. Since most of the incident photons are discarded by detectors, SPECT has a much lower sensitivity (by 1 to 2 orders of magnitude) than PET.

Several $^{99m}$Tc- or $^{111}$In-labeled murine mAbs have been approved by the FDA for use in SPECT imaging [48]. For instance, capromab pendetide labeled by $^{111}$In is a radioactive mAb against prostate-specific membrane antigen. Coupled with improved techniques in anatomic localization, SPECT via this radiolabeled mAb accurately localized soft tissue metastasis in prostate cancer patients [89]. Although there is few clinical trials for SPECT imaging using HER-2 targeting antibodies, related studies using SPECT/CT have been reported in mouse xenografts [90, 91]. After screening a set of nanobodies, 2Rs15d was selected, which is stable, specific, and does not compete with trastuzumab or pertuzumab in HER-2 targeting. As a result, $^{99m}$Tc-labeled 2Rs15d exhibited high uptake in HER-2 positive mouse tumor models, with fast blood clearance, high tumor-to-blood/muscle ratios, and low background in normal tissues [90] (Fig. (3)). Similar studies were carried out with an $^{111}$In-labeled albumin-binding Fab, AB.Fab4D5, which was derived from trastuzumab and exhibited rapid targeting, excellent tumor accumulation and retention [91]. With respect to individual SPECT or CT images, the fused images were advantageous in assessing potential bone metastases and differentiating malignant from benign bone lesions [92].

## MAGNETIC RESONANCE IMAGING (MRI)

MRI detects nuclei of atoms inside the body based on their nuclear magnetic resonance. The signal of MRI depends on the longitudinal ($T_1$) and transverse ($T_2$) relaxation times of protons mostly from tissue water, whose relaxation differences result in different MRI contrast [93]. The relaxation time of tissue water is affected by its physiological environment, which only happens at a late stage of physiological process, and is not specific [93]. To achieve an early and specific detection, contrast agents that decrease the longitudinal and transverse relaxation time can be intravenously injected to enhance the appearance of blood vessels and tumors [93]. The relaxivity of these agents, $r_1$ or $r_2$, is defined based on their ability to decrease $T_1$ or $T_2$ relaxation time, respectively. MRI contrast agents are classified into two categories based on their $r_2/r_1$ ratios. The ones with a high $r_2/r_1$ ratio, such as iron oxide particles, can result in a negative contrast or dark spots in $T_2$-weighted images; while the ones with a low $r_2/r_1$ ratio, such as complexes of $Gd^{3+}$, or $Mn^{2+}$, generate a positive contrast or bright spot in $T_1$-weighted images [93].

Although MRI has a high spatial resolution [94], it has a low sensitivity that needs to be improved by contrast agents of a high relaxivity [93]. Gadolinium chelates were used in early studies where they were conjugated to antibodies as exogenous contrast agents [95] (Fig. (4)). However, $Gd^{3+}$ suffers from low relaxivity and biocompatibility, which makes the alternative superparamagnetic iron oxide (SPIO) particles more attractive in MRI applications [94]. Other than the advantage in relaxivity, SPIO also improves the sensitivity due to its inherent composition of a great number of iron atoms [94]. These irons are biocompatible and can be metabolized *in vivo*. In addition, SPIO particles possess easily modifiable surface coating, size-dependent magnetic property for derivatization, and optical/electronic active spectra for facile detection [94, 96]. SPIO nanoparticles are commonly synthesized via precipitation-based methods, either by co-precipitation or by the reverse micelle technique [97, 98]. To be suitable for passage through capillary walls and micro-distribution within the tumor tissue, the size of these particles should be below 50 nm [99]. After synthesis, the particles can be further coated with a PEG-modified, phospholipid micelle shell [98] or an amphiphilic lipid bilayer [93], both of which can improve water solubility, stability, and circulation retention time of the particle, and provide a versatile platform for conjugation of various functional moieties including antibodies [93, 98, 99]. Based on the applications and probe design, MRI contrast agents can be broadly divided into four classes: non-specific contrast agents, targeted contrast agents incorporating ligands for specific molecular targeting, smart contrast agents only activated by certain events such as enzymatic cleavage, and cell labeling contrast agents comprising ligands for cellular targeting [93]. In this review article, we will focus on antibody-based imaging which mainly involves targeted contrast agents and cell labeling contrast agents.

Using antibodies as the targeting ligands, SPIO-based noninvasive MRI imaging has been widely studied in oncology [100]. In several early reports, anti-HER-2 antibodies were conjugated to iron oxide containing nanoparticles and showed effective *in vitro* imaging of breast cancer cells via $T_2$-weighted MRI [101–103]. Through a process that involved systematic evaluation of the magnetic spin, size and type of spinel metal ferrites, artificially engineered magnetic nanoprobes (Mn-doped magnetism-engineered iron oxide; MnMEIO) linked to trastuzumab were shown to be able to visualize small tumors implanted in a mouse while trastuzumab conjugated cross-linked iron oxide (CLIO) does not [104]. Recently, trastuzumab-conjugated iron oxide nanoparticles were successfully utilized in mice bearing breast cancer tumor, where the tumor site was detected by $T_2$-weighted MRI (Fig. (4)) [105].

Besides intact antibodies, anti-HER-2 affibody was also labeled with SPIO, and demonstrated to be a feasible, specific MRI contrast agent which accumulated to human ovarian SKOV-3 tumor lesions in an *in vivo* model, and can be detected by MRI at around 30 min after probe injection [106]. Recently, a protein was designed to contain a $Gd^{3+}$ binding site, which exhibited a significantly improved $T_1$ relaxivity than other traditional MRI contrast agents [107]. Once conjugated with an anti-HER-2 affibody, the probe demonstrated a significant improvement in detecting HER-2 positive human cell lines both *in vitro* and in mouse xenograft models [107].

Although many clinical trials in patients with HER-2 expressing breast cancer involve MRI as the imaging/diagnostic tool [108, 109], there is no reported clinical use of a MRI contrast agent that is comprised of an anti-HER-2 antibody. Nonetheless, with the rapid development of antibody-based contrast agents, the clinical application is feasible and expected for antibody-based MRI of HER-2.

## NEAR-INFRARED FLUORESCENCE (NIRF) IMAGING

Optical imaging has been a vibrant research area over the last decade, which is suitable for preclinical research in small animal models and a variety of clinical scenarios [110–115]. Photon penetration through living tissues is subjected to attenuation by tissue absorption and scattering. Given that near-infrared (NIR, 700–900 nm) light is lowly absorbed in most tissue chromophores such as hemoglobins, NIR light can penetrate several centimeters of tissue and can thereby be clinically useful [116, 117]. In addition, significant auto-fluorescence of tissue severely compromises the signal to background ratio of optical imaging using visible light, which is, however, dramatically reduced in the NIR region [117].

Much progress has been made in recent years to use noninvasive NIRF imaging in diagnostics and image-guided drug delivery, even though the detection of deep and small lesions remains a challenge [116]. Commonly used contrast agents are organic small molecules such as indocyanine green (ICG, a NIR dye) which has been FDA-approved, IRDye78 (a tetra-sulfonated heptamethine indocyanine fluorophore), cyanine dyes (e.g. Cy5, Cy5.5, Cy7, etc), among others [116–118]. Antibodies can be readily conjugated to these organic fluorophores for tumor imaging. For example, Cy7-conjugated trastuzumab was mixed with other fluorescently labeled mAbs and injected to tumor-bearing mice [119]. With multi-filter spectrally resolved fluorescence imaging at 24 h after injection of the antibody cocktail, different tumor types in mice can be distinguished by separate fluorescence from their bound antibodies, including the HER-2 positive NIH3T3 tumors. Several other fluorophores, such as Cy5.5 [120, 121], AF750 [121], RhodG dye [122], ICG dye [123], IRDye 800CW [124] (Fig. (5)), and rhodamine green [125] have all been conjugated to trastuzumab for NIRF imaging of HER-2 in tumor-bearing mice. Among these, several studies further demonstrated NIRF imaging as a useful tool for monitoring the effects of trastuzumab therapy [19, 121], or to guide the surgical removal of tumor tissues [125]. Recently, with the use of mathematical modeling, Alexa Fluor®750 dye labeled $Z_{HER\text{-}2:342}$ based affibody was demonstrated to be useful for quantitative assessment of HER-2 expression *in vivo* [126].

Conventional organic fluorophores suffer from certain limitations, such as their untunable excitation and emission wavelengths, low quantum yields in aqueous solutions, photobleaching, and limited number of sites for conjugation of targeting ligands, all of which undermine the feasibility and sensitivity of NIRF imaging with fluorescent dyes [116]. Alternatively, nanomaterials such as quantum dot (QD), carbon nanotubes, and gold nanoshells, have been investigated as inorganic fluorophores [127–129]. Among them, QD is the most intensively studied due to its unique optical properties including broadband absorption, high quantum yield, and low photobleaching [117, 130]. In addition to the advantages in optics, as a nanoparticle, QD also possesses multi-valency for drug loading as well as the enhanced permeation and retention (EPR) effect that can potentially facilitate its use for drug delivery. A biocompatibility study of QDs and trastuzumab-conjugated QDs in rats revealed that antibody conjugation can significantly control the toxicity of QDs and make them suitable for breast cancer imaging [129]. To date, advanced *in vivo* experiments using QDs are still lacking [131], with most of the reported HER-2 imaging conducted at the cellular level. Among a number of reports using anti-HER-2 antibody labeled QDs [132–135], one study clearly demonstrated that QD-based immunofluorescence imaging was more sensitive and gave stronger signals than traditional techniques [133]. Therefore, anti-HER-2 antibody modified QDs are considered to be promising agents for delineating the heterogeneity of HER-2-positive tumors.

## PHOTOACOUSTIC TOMOGRAPHY (PAT)

Optical imaging techniques face challenges in imaging deep tissue, since biological tissues are always optically scattering, where most photons are unable to penetrate deeper than the optical transport mean free path (~ 1 mm) [136]. The spatial resolution of these imaging techniques is thereby largely impeded by the depth [137]. In addition to the aforementioned NIRF imaging, many other imaging approaches with kindles beyond optics are currently under development. Given that ultrasound scattering in soft tissues is two to three orders of magnitude weaker, it is believed that a better resolution can be achieved with ultrasound-based imaging, even at a depth greater than the optical transport mean free path [137]. Ultrasonography is an ultrasound-based medical imaging technique that relies on the acquisition, analysis, and display of acoustic signals generated by reflection or backscatter of sound at a frequency higher than the audible range of humans [138]. Ultrasound imaging without contrast agents suffers from weak contrast in its detection of mechanical properties of tissues, thereby much less sensitive than other imaging approaches [137]. Therefore, contrast agents such as microbubbles and polymeric particles have to be used in any cases for ultrasonography [137]. Recently, PAT was developed which overcame these limits by combining the strengths of optical imaging and ultrasound to achieve a good optical contrast and a high ultrasonic resolution in one single system for high-resolution imaging *in vivo* [136].

PAT is based on the photoacoustic effect, in which the tissue or organ generates acoustic waves after the absorption of electromagnetic energy such as radio-frequency or optical waves [136, 137]. The tissue is usually irradiated by a short pulsed electromagnetic wave/light/laser beam, upon the absorption of which acoustic transient pressure is raised as the initial source of acoustic waves, together with thermoelastic expansion. The photoacoustic waves reach the tissue surface with different time delays, and are recorded by ultrasonic transducers to map the spatial distribution of acoustic sources. The tunable ultrasonic bandwidth in PAT determines the imaging depth and the spatial resolution in the tissue, with a 10 MHz bandwidth for a 0.1 mm resolution [136, 137]. Since many diseases do not possess enough endogenous photoacoustic contrast, exogenous contrast agents are required to target the specific diseased regions for precise and enhanced PAT images.

To date, a number of nanoparticles have been described as contrast agents for PAT, such as iron oxide and gold-couple core-shell nanoparticles [139], gold nanorods [140, 141], and single-walled carbon nanotubes (SWNT) [142]. With antibody-conjugated nanoparticles, the functional and molecular activity of tumor cells and diseased tissues can be visualized by PAT. Gold nanoparticles conjugated with trastuzumab were demonstrated to selectively target human SKBR-3 breast cancer cells in a gelatin phantom resembling the breast tissue, where $1\times10^9$ nanoparticles were detected at a depth of 6 cm [143]. Anti-HER-2 antibodies were also conjugated to gold nanorods [144], nanoparticles made by biodegradable polyactic acid [145], or embedded with ICG dye [146] to investigate their capability to target breast cancer and prostate cancer cells *in vitro* with a high contrast and a high efficiency [146]. HER-2-targeted PAT imaging using gold nanorods was also conducted in the OECM1 tumor-bearing mouse, where the photoacoustic intensity within the tumor region raised to 3 dB higher than the pre-injection level, at around 30 min after injection (Fig. (6)) [147].

## MULTIMODALITY IMAGING

Each imaging modality discussed above possesses both advantages and disadvantages, in terms of the physical characteristics and the detection of the signals. Multimodality imaging can potentially combine the advantages of these modalities to overcome their respective disadvantages. For instance, optical imaging provides a direct, fast, low-cost, and real-time

screening for surface lesions. However, it suffers from a limited sensitivity in deep tissue and is not apt for quantitative and tomographic imaging. On the other hand, nuclear imaging is superior in deep tissue sensitivity and quantitative imaging, yet it can be at a higher cost and requires a more restricted target-specificity due to the always-on characteristics of ionizing radiation [148, 149].

Radiolabeled anti-HER-2 antibodies or antibody fragments have been employed in nuclear imaging, and the resulting images were fused with X-ray CT [1, 11]. The C6.5 diabody, after being labeled with radioiodine, exhibited a time-dependent HER-2-positive tumor targeting [77], and was used effectively with PET/CT to evaluate HER-2 levels in response to HER-2-directed therapeutic treatments [78]. Another example of dual-modality imaging is with combined SPECT/CT, which has been described previously. The fused SPECT/CT affords a clearer visualization and localization of radiotracers in mouse models, thereby facilitating the evaluation of their bio-distributions and specificity of tumor uptake [90, 91, 150, 151]. Besides CT, other optical imaging approaches have been conducted simultaneously with PET imaging, such as NIRF imaging. In one report, PET was used to verify the detection results of NIRF imaging, in which two antibody-based contrast agents for PET and NIRF imaging purposes were prepared accordingly [124]. Other than optical imaging, anti-HER-2 antibody-based PET was sometimes co-performed with MRI. The results of these two imaging approaches were cross-validated with each other, to confirm the position of radiolabeled antibody *in vivo* [80, 152]. Clinically, fusion images from PET/MRI were reported to facilitate the identification of previously undetected lesions and metastasis in patients [80].

Compared to contrast agents separately prepared for more than one modality, the development of a single contrast agent for multimodality imaging can allow for a better synchronized scan, and can minimize the errors/differences caused by different agents. Given the inherent multi-valency, nanoparticles are ideal platforms for multimodality imaging. The anti-HER-2 antibody coated water-soluble FePt nanoparticles were demonstrated to be biocompatible in mouse models and were applicable to CT/MRI imaging [153]. Other iron oxide nanoparticles were either labeled with anti-HER-2 antibodies pre-conjugated by fluorophores [154], or coated simultaneously with both fluorophores and HER-2 antibodies (Fig. (7)) [155], for both NIRF and MRI imaging in tumor-bearing mice. In addition, a streptavidin nanoparticle was reported to be modified simultaneously by biotinylated trastuzumab, Cy5.5 fluorophore, and a $^{111}$In labeled chelator, which collectively allowed for fluorescence and SPECT imaging in mice bearing HER-2-positive tumors [149]. Other than nanoparticles, anti-HER-2 antibodies can also be utilized to carry both radionuclides and fluorescent dyes for combined RIS/NIRF imaging [148, 156], or combined PET/NIRF imaging [157].

## CONCLUSION

We have summarized several essential imaging techniques in antibody-based imaging of HER-2, among which the most sensitive techniques appear to be radionuclide-based. One concern of radionuclide-based imaging is its potential radio-hazard that may cause adverse effects. Therefore, alternative imaging techniques are emerging, such as PAT that can combine the advantages of ultrasound and optical fluorescence. Other than these single modality imaging approaches, multimodality imaging has also attracted intensive research interests which combine the advantages and circumvent the disadvantages of each single approach. Due to the limited endogenous contrast, most of these imaging techniques rely on exogenous contrast agents to achieve the desired spatial resolution and contrast. Therefore, the development of antibody-based contrast agents remains a promising direction in image-guided diagnostics and therapy.

Antibody-based imaging of HER-2, especially quantitative imaging, is highly valuable at several stages of pharmaceutical development and therapeutic intervention. Preclinical imaging studies in animal models can reveal the efficiency of antibody drugs in tumor targeting and therapy. Clinical imaging in patients can be employed to determine the optimal antibody dosing for tumor targeting, to assess the toxicity based on nonspecific uptake in normal organs, and to reveal inter-patient variations in pharmacokinetics and pharmacodynamics. Importantly, biopsy of tumors is traditionally used to confirm antigen expression level and to select patients for HER-2 targeted therapy, which may not represent an overall *in vivo* HER-2 expression statussince tumors are highly heterogeneous and in many cases hardly accessible. Antibody-based imaging, in this regard, may have unique values for patient selection due to its noninvasive, quantitative, time-sensitive, and whole-body nature for the assessment of both tumors and normal tissues.

Currently, many clinical trials are ongoing for antibody-based imaging of HER-2, most of which make use of the FDA-approved trastuzumab (Table 1). It is notable that some clinical trials are already starting to use HER-2 imaging to evaluate the therapeutic effects of small molecule or antibody-based anticancer drugs. Among all available imaging techniques, PET appears to be the most useful/used in clinical trials for HER-2 imaging, presumably due to its excellent sensitivity and good imaging quality. Moreover, this diverse set of imaging techniques may be employed in future clinical studies, in the form of multimodality imaging, to complement with each other for validation purposes, and also for improved imaging sensitivity and resolution. Taken together, antibody-based HER-2 imaging has moved into the clinic, which is expected to make a significant impact in clinical patient management and personalized medicine in the near future.

## Acknowledgments

The authors acknowledge financial support from the University of Wisconsin Carbone Cancer Center, the Department of Defense (W81XWH-11-1-0644), the National Center for Advancing Translational Sciences (NCATS) grant 9U54TR000021, and the Elsa U. Pardee Foundation.

## References

1. Cai W, Niu G, Chen X. Multimodality imaging of the HER-kinase axis in cancer. Eur J Nucl Med Mol Imaging. 2008; 35:186–208. [PubMed: 17846765]
2. Casalini P, Iorio MV, Galmozzi E, Menard S. Role of HER receptors family in development and differentiation. J Cell Physiol. 2004; 200:343–50. [PubMed: 15254961]
3. Mass RD. The HER receptor family: a rich target for therapeutic development. Int J Radiat Oncol Biol Phys. 2004; 58:932–40. [PubMed: 14967453]
4. Tai W, Mahato R, Cheng K. The role of HER2 in cancer therapy and targeted drug delivery. J Control Release. 2010; 146:264–75. [PubMed: 20385184]
5. Rubin I, Yarden Y. The basic biology of HER2. Ann Oncol. 2001; 12 (Suppl 1):S3–8. [PubMed: 11521719]
6. Meric-Bernstam F, Hung MC. Advances in targeting human epidermal growth factor receptor-2 signaling for cancer therapy. Clin Cancer Res. 2006; 12:6326–30. [PubMed: 17085641]
7. Bacus SS, Ruby SG, Weinberg DS, et al. HER-2/neu oncogene expression and proliferation in breast cancers. Am J Pathol. 1990; 137:103–11. [PubMed: 1973597]
8. Tan M, Yao J, Yu D. Overexpression of the c-erbB-2 gene enhanced intrinsic metastasis potential in human breast cancer cells without increasing their transformation abilities. Cancer Res. 1997; 57:1199–205. [PubMed: 9067293]
9. Bargmann CI, Hung MC, Weinberg RA. Multiple independent activations of the neu oncogene by a point mutation altering the transmembrane domain of p185. Cell. 1986; 45:649–57. [PubMed: 2871941]

10. Schechter AL, Hung MC, Vaidyanathan L, et al. The neu gene: an erbB-homologous gene distinct from and unlinked to the gene encoding the EGF receptor. Science. 1985; 229:976–8. [PubMed: 2992090]
11. Niu G, Cai W, Chen X. Molecular imaging of human epidermal growth factor receptor 2 (HER-2) expression. Front Biosci. 2008; 13:790–805. [PubMed: 17981588]
12. Hofer A, Saez JC, Chang CC, et al. C-erbB2/neu transfection induces gap junctional communication incompetence in glial cells. J Neurosci. 1996; 16:4311–21. [PubMed: 8699242]
13. Schneider PM, Hung MC, Chiocca SM, et al. Differential expression of the c-erbB-2 gene in human small cell and non-small cell lung cancer. Cancer Res. 1989; 49:4968–71. [PubMed: 2569928]
14. Slamon DJ, Godolphin W, Jones LA, et al. Studies of the HER-2/neu proto-oncogene in human breast and ovarian cancer. Science. 1989; 244:707–12. [PubMed: 2470152]
15. Park JW, Stagg R, Lewis GD, et al. Anti-p185HER2 monoclonal antibodies: biological properties and potential for immunotherapy. Cancer Treat Res. 1992; 61:193–211. [PubMed: 1360232]
16. Agus DB, Akita RW, Fox WD, et al. Targeting ligand-activated ErbB2 signaling inhibits breast and prostate tumor growth. Cancer Cell. 2002; 2:127–37. [PubMed: 12204533]
17. Agus DB, Gordon MS, Taylor C, et al. Phase I clinical study of pertuzumab, a novel HER dimerization inhibitor, in patients with advanced cancer. J Clin Oncol. 2005; 23:2534–43. [PubMed: 15699478]
18. Nahta R, Hung MC, Esteva FJ. The HER-2-targeting antibodies trastuzumab and pertuzumab synergistically inhibit the survival of breast cancer cells. Cancer Res. 2004; 64:2343–6. [PubMed: 15059883]
19. Scheuer W, Friess T, Burtscher H, et al. Strongly enhanced antitumor activity of trastuzumab and pertuzumab combination treatment on HER2-positive human xenograft tumor models. Cancer Res. 2009; 69:9330–6. [PubMed: 19934333]
20. Konecny GE, Pegram MD, Venkatesan N, et al. Activity of the dual kinase inhibitor lapatinib (GW572016) against HER-2-overexpressing and trastuzumab-treated breast cancer cells. Cancer Res. 2006; 66:1630–9. [PubMed: 16452222]
21. Drummond DC, Marx C, Guo Z, et al. Enhanced pharmacodynamic and antitumor properties of a histone deacetylase inhibitor encapsulated in liposomes or ErbB2-targeted immunoliposomes. Clin Cancer Res. 2005; 11:3392–401. [PubMed: 15867240]
22. Solit DB, Zheng FF, Drobnjak M, et al. 17-Allylamino-17-demethoxygeldanamycin induces the degradation of androgen receptor and HER-2/neu and inhibits the growth of prostate cancer xenografts. Clin Cancer Res. 2002; 8:986–93. [PubMed: 12006510]
23. Tan WB, Jiang S, Zhang Y. Quantum-dot based nanoparticles for targeted silencing of HER2/neu gene via RNA interference. Biomaterials. 2007; 28:1565–71. [PubMed: 17161865]
24. Thybusch-Bernhardt A, Aigner A, Beckmann S, Czubayko F, Juhl H. Ribozyme targeting of HER-2 inhibits pancreatic cancer cell growth in vivo. Eur J Cancer. 2001; 37:1688–94. [PubMed: 11527697]
25. Bast RC Jr, Ravdin P, Hayes DF, et al. 2000 update of recommendations for the use of tumor markers in breast and colorectal cancer: clinical practice guidelines of the American Society of Clinical Oncology. J Clin Oncol. 2001; 19:1865–78. [PubMed: 11251019]
26. Junqueira, LCU.; Carneiro, J.; Contopoulos, AN. Basic histology. Los Altos, Calif: Lange Medical Publications; 1975.
27. Wilder RB, DeNardo GL, DeNardo SJ. Radioimmunotherapy: recent results and future directions. J Clin Oncol. 1996; 14:1383–400. [PubMed: 8648397]
28. Holliger P, Hudson PJ. Engineered antibody fragments and the rise of single domains. Nat Biotechnol. 2005; 23:1126–36. [PubMed: 16151406]
29. Vuillez JP, Peltier P, Caravel JP, et al. Immunoscintigraphy using 111In-labeled F(ab′)2 fragments of anticarcinoembryonic antigen monoclonal antibody for detecting recurrences of medullary thyroid carcinoma. J Clin Endocrinol Metab. 1992; 74:157–63. [PubMed: 1727816]
30. Kohler G, Milstein C. Continuous cultures of fused cells secreting antibody of predefined specificity. Nature. 1975; 256:495–7. [PubMed: 1172191]

31. Reichert JM, Rosensweig CJ, Faden LB, Dewitz MC. Monoclonal antibody successes in the clinic. Nat Biotechnol. 2005; 23:1073–8. [PubMed: 16151394]
32. Stern M, Herrmann R. Overview of monoclonal antibodies in cancer therapy: present and promise. Crit Rev Oncol Hematol. 2005; 54:11–29. [PubMed: 15780905]
33. Roovers RC, van Dongen GA, van Bergen en Henegouwen PM. Nanobodies in therapeutic applications. Curr Opin Mol Ther. 2007; 9:327–35. [PubMed: 17694445]
34. Nord K, Gunneriusson E, Ringdahl J, et al. Binding proteins selected from combinatorial libraries of an alpha-helical bacterial receptor domain. Nat Biotechnol. 1997; 15:772–7. [PubMed: 9255793]
35. Beste G, Schmidt FS, Stibora T, Skerra A. Small antibody-like proteins with prescribed ligand specificities derived from the lipocalin fold. Proc Natl Acad Sci U S A. 1999; 96:1898–903. [PubMed: 10051566]
36. Nilsson B, Moks T, Jansson B, et al. A synthetic IgG-binding domain based on staphylococcal protein A. Protein Eng. 1987; 1:107–13. [PubMed: 3507693]
37. Nord K, Nilsson J, Nilsson B, Uhlen M, Nygren PA. A combinatorial library of an alpha-helical bacterial receptor domain. Protein Eng. 1995; 8:601–8. [PubMed: 8532685]
38. Wikman M, Steffen AC, Gunneriusson E, et al. Selection and characterization of HER2/neu-binding affibody ligands. Protein Eng Des Sel. 2004; 17:455–62. [PubMed: 15208403]
39. Reichert JM. Monoclonal antibodies as innovative therapeutics. Curr Pharm Biotechnol. 2008; 9:423–30. [PubMed: 19075682]
40. Alley SC, Okeley NM, Senter PD. Antibody-drug conjugates: targeted drug delivery for cancer. Curr Opin Chem Biol. 2010; 14:529–37. [PubMed: 20643572]
41. McDonagh CF, Turcott E, Westendorf L, et al. Engineered antibody-drug conjugates with defined sites and stoichiometries of drug attachment. Protein Eng Des Sel. 2006; 19:299–307. [PubMed: 16644914]
42. Sun MM, Beam KS, Cerveny CG, et al. Reduction-alkylation strategies for the modification of specific monoclonal antibody disulfides. Bioconjug Chem. 2005; 16:1282–90. [PubMed: 16173809]
43. Junutula JR, Raab H, Clark S, et al. Site-specific conjugation of a cytotoxic drug to an antibody improves the therapeutic index. Nat Biotechnol. 2008; 26:925–32. [PubMed: 18641636]
44. Smith GP. Filamentous fusion phage: novel expression vectors that display cloned antigens on the virion surface. Science. 1985; 228:1315–7. [PubMed: 4001944]
45. Jain RK. Barriers to drug delivery in solid tumors. Sci Am. 1994; 271:58–65. [PubMed: 8066425]
46. Keane TE, Rosner IL, Wingo MS, McLeod DG. The emergence of radioimmunoscintigraphy for prostate cancer. Rev Urol. 2006; 8 (Suppl 1):S20–8. [PubMed: 17021623]
47. de Bree R, Roos JC, Quak JJ, et al. Clinical imaging of head and neck cancer with technetium-99m-labeled monoclonal antibody E48 IgG or F(ab′)2. J Nucl Med. 1994; 35:775–83. [PubMed: 8176458]
48. Zuckier LS, DeNardo GL. Trials and tribulations: oncological antibody imaging comes to the fore. Semin Nucl Med. 1997; 27:10–29. [PubMed: 9122720]
49. Kotts CE, Su FM, Leddy C, et al. 186Re-labeled antibodies to p185HER2 as HER2-targeted radioimmunopharmaceutical agents: comparison of physical and biological characteristics with 125I and 131I-labeled counterparts. Cancer Biother Radiopharm. 1996; 11:133–44. [PubMed: 10851530]
50. Tai MS, McCartney JE, Adams GP, et al. Targeting c-erbB-2 expressing tumors using single-chain Fv monomers and dimers. Cancer Res. 1995; 55:5983s–9s. [PubMed: 7493381]
51. Tang Y, Wang J, Scollard DA, et al. Imaging of HER2/neu-positive BT-474 human breast cancer xenografts in athymic mice using (111)In-trastuzumab (Herceptin) Fab fragments. Nucl Med Biol. 2005; 32:51–8. [PubMed: 15691661]
52. Steffen AC, Orlova A, Wikman M, et al. Affibody-mediated tumour targeting of HER-2 expressing xenografts in mice. Eur J Nucl Med Mol Imaging. 2006; 33:631–8. [PubMed: 16538504]

53. Orlova A, Tolmachev V, Pehrson R, et al. Synthetic affibody molecules: a novel class of affinity ligands for molecular imaging of HER2-expressing malignant tumors. Cancer Res. 2007; 67:2178–86. [PubMed: 17332348]
54. Ahlgren S, Orlova A, Wallberg H, et al. Targeting of HER2-expressing tumors using 111In-ABY-025, a second-generation affibody molecule with a fundamentally reengineered scaffold. J Nucl Med. 2010; 51:1131–8. [PubMed: 20554729]
55. Tran T, Engfeldt T, Orlova A, et al. (99m)Tc-maEEE-Z(HER2:342), an Affibody molecule-based tracer for the detection of HER2 expression in malignant tumors. Bioconjug Chem. 2007; 18:1956–64. [PubMed: 17944527]
56. Wong JY, Raubitschek A, Yamauchi D, et al. A pretherapy biodistribution and dosimetry study of indium-111-radiolabeled trastuzumab in patients with human epidermal growth factor receptor 2-overexpressing breast cancer. Cancer Biother Radiopharm. 2010; 25:387–94. [PubMed: 20707718]
57. Perik PJ, Lub-De Hooge MN, Gietema JA, et al. Indium-111-labeled trastuzumab scintigraphy in patients with human epidermal growth factor receptor 2-positive metastatic breast cancer. J Clin Oncol. 2006; 24:2276–82. [PubMed: 16710024]
58. Alauddin MM. Positron emission tomography (PET) imaging with $^{18}$F-based radiotracers. Am J Nucl Med Mol Imaging. 2012; 2:55–76. [PubMed: 23133802]
59. Cai W, Hong H. Peptoid and positron emission tomography: an appealing combination. Am J Nucl Med Mol Imaging. 2011; 1:76–9. [PubMed: 22022661]
60. Eary JF, Hawkins DS, Rodler ET, Conrad EUI. $^{18}$F-FDG PET in sarcoma treatment response imaging. Am J Nucl Med Mol Imaging. 2011; 1:47–53. [PubMed: 23133794]
61. Grassi I, Nanni C, Allegri V, et al. The clinical use of PET with $^{11}$C-acetate. Am J Nucl Med Mol Imaging. 2012; 2:33–47. [PubMed: 23133801]
62. Iagaru A. $^{18}$F-FDG PET/CT: timing for evaluation of response to therapy remains a clinical challenge. Am J Nucl Med Mol Imaging. 2011; 1:63–4. [PubMed: 23133796]
63. Vach W, Høilund-Carlsen PF, Fischer BM, Gerke O, Weber W. How to study optimal timing of PET/CT for monitoring of cancer treatment. Am J Nucl Med Mol Imaging. 2011; 1:54–62. [PubMed: 23133795]
64. Phelps, ME. PET : physics, instrumentation, and scanners. New York ; Berlin: Springer; 2006.
65. van Dongen GA, Vosjan MJ. Immuno-positron emission tomography: shedding light on clinical antibody therapy. Cancer Biother Radiopharm. 2010; 25:375–85. [PubMed: 20707716]
66. Verel I, Visser GW, van Dongen GA. The promise of immuno-PET in radioimmunotherapy. J Nucl Med. 2005; 46 (Suppl 1):164S–71S. [PubMed: 15653665]
67. McCabe KE, Wu AM. Positive progress in immunoPET--not just a coincidence. Cancer Biother Radiopharm. 2010; 25:253–61. [PubMed: 20578830]
68. Zhang Y, Cai W. Molecular imaging of insulin-like growth factor 1 receptor in cancer. Am J Nucl Med Mol Imaging. 2012; 2:248–59. [PubMed: 23066521]
69. Zhang Y, Hong H, Engle JW, et al. Positron emission tomography and near-infrared fluorescence imaging of vascular endothelial growth factor with dual-labeled bevacizumab. Am J Nucl Med Mol Imaging. 2012; 2:1–13. [PubMed: 22229128]
70. Olafsen T, Kenanova VE, Sundaresan G, et al. Optimizing radiolabeled engineered anti-p185HER2 antibody fragments for in vivo imaging. Cancer Res. 2005; 65:5907–16. [PubMed: 15994969]
71. Tinianow JN, Gill HS, Ogasawara A, et al. Site-specifically 89Zr-labeled monoclonal antibodies for ImmunoPET. Nucl Med Biol. 2010; 37:289–97. [PubMed: 20346868]
72. Paudyal P, Paudyal B, Hanaoka H, et al. Imaging and biodistribution of Her2/neu expression in non-small cell lung cancer xenografts with Cu-labeled trastuzumab PET. Cancer Sci. 2010; 101:1045–50. [PubMed: 20219072]
73. Oude Munnink TH, Korte MA, Nagengast WB, et al. (89)Zr-trastuzumab PET visualises HER2 downregulation by the HSP90 inhibitor NVP-AUY922 in a human tumour xenograft. Eur J Cancer. 2010; 46:678–84. [PubMed: 20036116]

74. Orlova A, Wallberg H, Stone-Elander S, Tolmachev V. On the selection of a tracer for PET imaging of HER2-expressing tumors: direct comparison of a 124I-labeled affibody molecule and trastuzumab in a murine xenograft model. J Nucl Med. 2009; 50:417–25. [PubMed: 19223403]
75. Wang RE. Targeting heat shock proteins 70/90 and proteasome for cancer therapy. Curr Med Chem. 2011; 18:4250–64. [PubMed: 21838681]
76. Adams GP, Schier R, McCall AM, et al. Prolonged in vivo tumour retention of a human diabody targeting the extracellular domain of human HER2/neu. Br J Cancer. 1998; 77:1405–12. [PubMed: 9652755]
77. Robinson MK, Doss M, Shaller C, et al. Quantitative immuno-positron emission tomography imaging of HER2-positive tumor xenografts with an iodine-124 labeled anti-HER2 diabody. Cancer Res. 2005; 65:1471–8. [PubMed: 15735035]
78. Reddy S, Shaller CC, Doss M, et al. Evaluation of the anti-HER2 C6.5 diabody as a PET radiotracer to monitor HER2 status and predict response to trastuzumab treatment. Clin Cancer Res. 2010; 17:1509–20. [PubMed: 21177408]
79. Dijkers EC, Kosterink JG, Rademaker AP, et al. Development and characterization of clinical-grade 89Zr-trastuzumab for HER2/neu immunoPET imaging. J Nucl Med. 2009; 50:974–81. [PubMed: 19443585]
80. Dijkers EC, Oude Munnink TH, Kosterink JG, et al. Biodistribution of 89Zr-trastuzumab and PET imaging of HER2-positive lesions in patients with metastatic breast cancer. Clin Pharmacol Ther. 2010; 87:586–92. [PubMed: 20357763]
81. Oude Munnink TH, Dijkers EC, Netters SJ, et al. Trastuzumab pharmacokinetics influenced by extent human epidermal growth factor receptor 2-positive tumor load. J Clin Oncol. 2010; 28:e355–6. author reply e7. [PubMed: 20458048]
82. Knoll GF. Single-Photon Emission Computed Tomography. Proc IEEE Inst Electr Electron Eng. 1983; 71:320.
83. Sharkey RM, Karacay H, McBride WJ, et al. Bispecific antibody pretargeting of radionuclides for immuno single-photon emission computed tomography and immuno positron emission tomography molecular imaging: an update. Clin Cancer Res. 2007; 13:5577s–85s. [PubMed: 17875792]
84. Aparici CM, Carlson D, Nguyen N, Hawkins RA, Seo Y. Combined SPECT and Multidetector CT for Prostate Cancer Evaluations. Am J Nucl Med Mol Imaging. 2012; 2:48–54. [PubMed: 22267999]
85. Bhargava P, He G, Samarghandi A, Delpassand ES. Pictorial review of SPECT/CT imaging applications in clinical nuclear medicine. Am J Nucl Med Mol Imaging. 2012; 2:221–31. [PubMed: 23133813]
86. Buckle T, van den Berg NS, Kuil J, et al. Non-invasive longitudinal imaging of tumor progression using an $^{111}$indium labeled CXCR4 peptide antagonist. Am J Nucl Med Mol Imaging. 2012; 2:99–109. [PubMed: 23133805]
87. Ogasawara Y, Ogasawara K, Suzuki T, et al. Preoperative $^{123}$I-iomazenil SPECT imaging predicts cerebral hyperperfusion following endarterectomy for unilateral cervical internal carotid artery stenosis. Am J Nucl Med Mol Imaging. 2012; 2:77–87. [PubMed: 23133803]
88. Zhao R, Wang J, Deng J, Yang W, Wang J. Efficacy of $^{99m}$Tc-EDDA/HYNIC-TOC SPECT/CT scintigraphy in Graves' ophthalmopathy. Am J Nucl Med Mol Imaging. 2012; 2:242–7. [PubMed: 23133815]
89. Taneja SS. ProstaScint(R) Scan: Contemporary Use in Clinical Practice. Rev Urol. 2004; 6 (Suppl 10):S19–28. [PubMed: 16985928]
90. Vaneycken I, Devoogdt N, Van Gassen N, et al. Preclinical screening of anti-HER2 nanobodies for molecular imaging of breast cancer. Faseb J. 2011; 25:2433–46. [PubMed: 21478264]
91. Dennis MS, Jin H, Dugger D, et al. Imaging tumors with an albumin-binding Fab, a novel tumor-targeting agent. Cancer Res. 2007; 67:254–61. [PubMed: 17210705]
92. Utsunomiya D, Shiraishi S, Imuta M, et al. Added value of SPECT/CT fusion in assessing suspected bone metastasis: comparison with scintigraphy alone and nonfused scintigraphy and CT. Radiology. 2006; 238:264–71. [PubMed: 16304081]

93. Mulder WJ, Strijkers GJ, van Tilborg GA, Griffioen AW, Nicolay K. Lipid-based nanoparticles for contrast-enhanced MRI and molecular imaging. NMR Biomed. 2006; 19:142–64. [PubMed: 16450332]
94. Bulte JW, Kraitchman DL. Iron oxide MR contrast agents for molecular and cellular imaging. NMR Biomed. 2004; 17:484–99. [PubMed: 15526347]
95. Sipkins DA, Cheresh DA, Kazemi MR, et al. Detection of tumor angiogenesis in vivo by alphaVbeta3-targeted magnetic resonance imaging. Nat Med. 1998; 4:623–6. [PubMed: 9585240]
96. Moore A, Weissleder R, Bogdanov A Jr. Uptake of dextran-coated monocrystalline iron oxides in tumor cells and macrophages. J Magn Reson Imaging. 1997; 7:1140–5. [PubMed: 9400860]
97. Shen T, Weissleder R, Papisov M, Bogdanov A Jr, Brady TJ. Monocrystalline iron oxide nanocompounds (MION): physicochemical properties. Magn Reson Med. 1993; 29:599–604. [PubMed: 8505895]
98. Nitin N, LaConte LE, Zurkiya O, Hu X, Bao G. Functionalization and peptide-based delivery of magnetic nanoparticles as an intracellular MRI contrast agent. J Biol Inorg Chem. 2004; 9:706–12. [PubMed: 15232722]
99. Tiefenauer LX, Tschirky A, Kuhne G, Andres RY. In vivo evaluation of magnetite nanoparticles for use as a tumor contrast agent in MRI. Magn Reson Imaging. 1996; 14:391–402. [PubMed: 8782177]
100. Peng XH, Qian X, Mao H, et al. Targeted magnetic iron oxide nanoparticles for tumor imaging and therapy. Int J Nanomedicine. 2008; 3:311–21. [PubMed: 18990940]
101. Funovics MA, Kapeller B, Hoeller C, et al. MR imaging of the her2/neu and 9.2.27 tumor antigens using immunospecific contrast agents. Magn Reson Imaging. 2004; 22:843–50. [PubMed: 15234453]
102. Lee J, Yang J, Seo SB, et al. Smart nanoprobes for ultrasensitive detection of breast cancer via magnetic resonance imaging. Nanotechnology. 2008; 19:485101. [PubMed: 21836291]
103. Yang HM, Park CW, Woo MA, et al. HER2/neu Antibody Conjugated Poly(amino acid)-Coated Iron Oxide Nanoparticles for Breast Cancer MR Imaging. Biomacromolecules. 2010; 11:2866–72.
104. Lee JH, Huh YM, Jun YW, et al. Artificially engineered magnetic nanoparticles for ultra-sensitive molecular imaging. Nat Med. 2007; 13:95–9. [PubMed: 17187073]
105. Chen TJ, Cheng TH, Chen CY, et al. Targeted Herceptin-dextran iron oxide nanoparticles for noninvasive imaging of HER2/neu receptors using MRI. J Biol Inorg Chem. 2009; 14:253–60. [PubMed: 18975017]
106. Kinoshita M, Yoshioka Y, Okita Y, Hashimoto N, Yoshimine T. MR molecular imaging of HER-2 in a murine tumor xenograft by SPIO labeling of anti-HER-2 affibody. Contrast Media Mol Imaging. 2010; 5:18–22. [PubMed: 20140973]
107. Qiao J, Li S, Wei L, et al. HER2 targeted molecular MR imaging using a de novo designed protein contrast agent. PLoS One. 2011; 6:e18103. [PubMed: 21455310]
108. Fischer U, Kopka L, Brinck U, et al. Prognostic value of contrast-enhanced MR mammography in patients with breast cancer. Eur Radiol. 1997; 7:1002–5. [PubMed: 9265662]
109. Niwinska A, Tacikowska M, Murawska M. The effect of early detection of occult brain metastases in HER2-positive breast cancer patients on survival and cause of death. Int J Radiat Oncol Biol Phys. 2010; 77:1134–9. [PubMed: 19932944]
110. Cai W, Zhang Y, Kamp TJ. Imaging of induced pluripotent stem cells: from cellular reprogramming to transplantation. Am J Nucl Med Mol Imaging. 2011; 1:18–28. [PubMed: 21841970]
111. Chin PTK, Beekman CAC, Buckle T, Josephson L, van Leeuwen FWB. Multispectral visualization of surgical safety-margins using fluorescent marker seeds. Am J Nucl Med Mol Imaging. 2012; 2:151–62. [PubMed: 23133810]
112. Huang X, Lee S, Chen X. Design of “smart” probes for optical imaging of apoptosis. Am J Nucl Med Mol Imaging. 2011; 1:3–17. [PubMed: 22514789]
113. Thorek DLJ, Robertson R, Bacchus WA, et al. Cerenkov imaging - a new modality for molecular imaging. Am J Nucl Med Mol Imaging. 2012; 2:163–73. [PubMed: 23133811]

114. Yigit MV, Medarova Z. In vivo and ex vivo applications of gold nanoparticles for biomedical SERS imaging. Am J Nucl Med Mol Imaging. 2012; 2:232–41. [PubMed: 23133814]
115. Sun M, Hoffman D, Sundaresan G, et al. Synthesis and characterization of intrinsically radio-labeled quantum dots for bimodal detection. Am J Nucl Med Mol Imaging. 2012; 2:122–35. [PubMed: 23133807]
116. Sevick-Muraca EM, Houston JP, Gurfinkel M. Fluorescence-enhanced, near infrared diagnostic imaging with contrast agents. Curr Opin Chem Biol. 2002; 6:642–50. [PubMed: 12413549]
117. Frangioni JV. In vivo near-infrared fluorescence imaging. Curr Opin Chem Biol. 2003; 7:626–34. [PubMed: 14580568]
118. Zaheer A, Lenkinski RE, Mahmood A, et al. In vivo near-infrared fluorescence imaging of osteoblastic activity. Nat Biotechnol. 2001; 19:1148–54. [PubMed: 11731784]
119. Koyama Y, Barrett T, Hama Y, et al. In vivo molecular imaging to diagnose and subtype tumors through receptor-targeted optically labeled monoclonal antibodies. Neoplasia. 2007; 9:1021–9. [PubMed: 18084609]
120. Hilger I, Leistner Y, Berndt A, et al. Near-infrared fluorescence imaging of HER-2 protein over-expression in tumour cells. Eur Radiol. 2004; 14:1124–9. [PubMed: 15118831]
121. Gee MS, Upadhyay R, Bergquist H, et al. Human breast cancer tumor models: molecular imaging of drug susceptibility and dosing during HER2/neu-targeted therapy. Radiology. 2008; 248:925–35. [PubMed: 18647846]
122. Koyama Y, Hama Y, Urano Y, et al. Spectral fluorescence molecular imaging of lung metastases targeting HER2/neu. Clin Cancer Res. 2007; 13:2936–45. [PubMed: 17504994]
123. Ogawa M, Kosaka N, Choyke PL, Kobayashi H. In vivo molecular imaging of cancer with a quenching near-infrared fluorescent probe using conjugates of monoclonal antibodies and indocyanine green. Cancer Res. 2009; 69:1268–72. [PubMed: 19176373]
124. Terwisscha van Scheltinga AG, van Dam GM, Nagengast WB, et al. Intraoperative near-infrared fluorescence tumor imaging with vascular endothelial growth factor and human epidermal growth factor receptor 2 targeting antibodies. J Nucl Med. 2011; 52:1778–85. [PubMed: 21990576]
125. Longmire M, Kosaka N, Ogawa M, Choyke PL, Kobayashi H. Multicolor in vivo targeted imaging to guide real-time surgery of HER2-positive micrometastases in a two-tumor coincident model of ovarian cancer. Cancer Sci. 2009; 100:1099–104. [PubMed: 19302283]
126. Chernomordik V, Hassan M, Lee SB, et al. Quantitative analysis of Her2 receptor expression in vivo by near-infrared optical imaging. Mol Imaging. 2010; 9:192–200. [PubMed: 20643022]
127. Bickford LR, Agollah G, Drezek R, Yu TK. Silica-gold nanoshells as potential intraoperative molecular probes for HER2-overexpression in ex vivo breast tissue using near-infrared reflectance confocal microscopy. Breast Cancer Res Treat. 2010; 120:547–55. [PubMed: 19418216]
128. Welsher K, Liu Z, Daranciang D, Dai H. Selective probing and imaging of cells with single walled carbon nanotubes as near-infrared fluorescent molecules. Nano Lett. 2008; 8:586–90. [PubMed: 18197719]
129. Tiwari DK, Jin T, Behari J. Bio-distribution and toxicity assessment of intravenously injected anti-HER2 antibody conjugated CdSe/ZnS quantum dots in Wistar rats. Int J Nanomedicine. 2011; 6:463–75. [PubMed: 21499435]
130. Lim YT, Kim S, Nakayama A, et al. Selection of quantum dot wavelengths for biomedical assays and imaging. Mol Imaging. 2003; 2:50–64. [PubMed: 12926237]
131. Tada H, Higuchi H, Wanatabe TM, Ohuchi N. *In vivo* real-time tracking of single quantum dots conjugated with monoclonal anti-HER2 antibody in tumors of mice. Cancer Res. 2007; 67:1138–44. [PubMed: 17283148]
132. Barat B, Sirk SJ, McCabe KE, et al. Cys-diabody quantum dot conjugates (immunoQdots) for cancer marker detection. Bioconjug Chem. 2009; 20:1474–81. [PubMed: 19642689]
133. Chen C, Peng J, Xia H, et al. Quantum-dot-based immunofluorescent imaging of HER2 and ER provides new insights into breast cancer heterogeneity. Nanotechnology. 2010; 21:095101. [PubMed: 20110584]

134. Liu XL, Peng CW, Chen C, et al. Quantum dots-based double-color imaging of HER2 positive breast cancer invasion. Biochem Biophys Res Commun. 2011; 409:577–82. [PubMed: 21609713]
135. Wu X, Liu H, Liu J, et al. Immunofluorescent labeling of cancer marker Her2 and other cellular targets with semiconductor quantum dots. Nat Biotechnol. 2003; 21:41–6. [PubMed: 12459735]
136. Wang LV. Prospects of photoacoustic tomography. Med Phys. 2008; 35:5758–67. [PubMed: 19175133]
137. Xu M, Wang L. Photoacoustic imaging in biomedicine. Rev Sci Instrum. 2006; 77:041101–22.
138. Lindner JR. Microbubbles in medical imaging: current applications and future directions. Nat Rev Drug Discov. 2004; 3:527–32. [PubMed: 15173842]
139. Jin Y, Jia C, Huang SW, O'Donnell M, Gao X. Multifunctional nanoparticles as coupled contrast agents. Nat Commun. 2010; 1:41. [PubMed: 20975706]
140. Chamberland DL, Agarwal A, Kotov N, et al. Photoacoustic tomography of joints aided by an Etanercept-conjugated gold nanoparticle contrast agent-an ex vivo preliminary rat study. Nanotechnology. 2008; 19:095101. [PubMed: 21817663]
141. Ha, S.; Kim, JS.; Tripathy, S., et al. Simultaneous photoacoustic detection of multiple inflammatory biomarkers using bioconjugated gold nanorods as selective targeting agents. Ultra Symp (IUS); 2010; IEEE; 2010.
142. de la Zerda A, Liu Z, Bodapati S, et al. Ultrahigh sensitivity carbon nanotube agents for photoacoustic molecular imaging in living mice. Nano Lett. 2010; 10:2168–72. [PubMed: 20499887]
143. Copland JA, Eghtedari M, Popov VL, et al. Bioconjugated gold nanoparticles as a molecular based contrast agent: implications for imaging of deep tumors using optoacoustic tomography. Mol Imaging Biol. 2004; 6:341–9. [PubMed: 15380744]
144. Li PC, Wei CW, Liao CK, et al. Photoacoustic imaging of multiple targets using gold nanorods. IEEE Trans Ultrason Ferroelectr Freq Control. 2007; 54:1642–7. [PubMed: 17703668]
145. Liu J, Li J, Rosol TJ, Pan X, Voorhees JL. Biodegradable nanoparticles for targeted ultrasound imaging of breast cancer cells in vitro. Phys Med Biol. 2007; 52:4739–47. [PubMed: 17671332]
146. Kim G, Huang SW, Day KC, et al. Indocyanine-green-embedded PEBBLEs as a contrast agent for photoacoustic imaging. J Biomed Opt. 2007; 12:044020. [PubMed: 17867824]
147. Li PC, Wang CR, Shieh DB, et al. In vivo photoacoustic molecular imaging with simultaneous multiple selective targeting using antibody-conjugated gold nanorods. Opt Express. 2008; 16:18605–15. [PubMed: 19581946]
148. Ogawa M, Regino CA, Seidel J, et al. Dual-modality molecular imaging using antibodies labeled with activatable fluorescence and a radionuclide for specific and quantitative targeted cancer detection. Bioconjug Chem. 2009; 20:2177–84. [PubMed: 19919110]
149. Liang M, Liu X, Cheng D, et al. Multimodality nuclear and fluorescence tumor imaging in mice using a streptavidin nanoparticle. Bioconjug Chem. 2010; 21:1385–8. [PubMed: 20557066]
150. Chen KT, Lee TW, Lo JM. In vivo examination of (188)Re(I)-tricarbonyl-labeled trastuzumab to target HER2-overexpressing breast cancer. Nucl Med Biol. 2009; 36:355–61. [PubMed: 19423002]
151. McLarty K, Cornelissen B, Cai Z, et al. Micro-SPECT/CT with 111In-DTPA-pertuzumab sensitively detects trastuzumab-mediated HER2 downregulation and tumor response in athymic mice bearing MDA-MB-361 human breast cancer xenografts. J Nucl Med. 2009; 50:1340–8. [PubMed: 19617342]
152. Palm S, Enmon RM Jr, Matei C, et al. Pharmacokinetics and Biodistribution of (86)Y-Trastuzumab for (90)Y dosimetry in an ovarian carcinoma model: correlative MicroPET and MRI. J Nucl Med. 2003; 44:1148–55. [PubMed: 12843231]
153. Chou SW, Shau YH, Wu PC, et al. In vitro and in vivo studies of FePt nanoparticles for dual modal CT/MRI molecular imaging. J Am Chem Soc. 2010; 132:13270–8. [PubMed: 20572667]
154. Corsi F, Fiandra L, De Palma C, et al. HER2 expression in breast cancer cells is downregulated upon active targeting by antibody-engineered multifunctional nanoparticles in mice. ACS Nano. 2011; 5:6383–93. [PubMed: 21790185]

155. Bardhan R, Chen W, Bartels M, et al. Tracking of Multimodal Therapeutic Nanocomplexes Targeting Breast Cancer in Vivo. Nano Lett. 2010; 10:4920–8.

156. Sampath L, Wang W, Sevick-Muraca EM. Near infrared fluorescent optical imaging for nodal staging. J Biomed Opt. 2008; 13:041312. [PubMed: 19021320]

157. Xu H, Eck PK, Baidoo KE, Choyke PL, Brechbiel MW. Toward preparation of antibody-based imaging probe libraries for dual-modality positron emission tomography and fluorescence imaging. Bioorg Med Chem. 2009; 17:5176–81. [PubMed: 19505829]

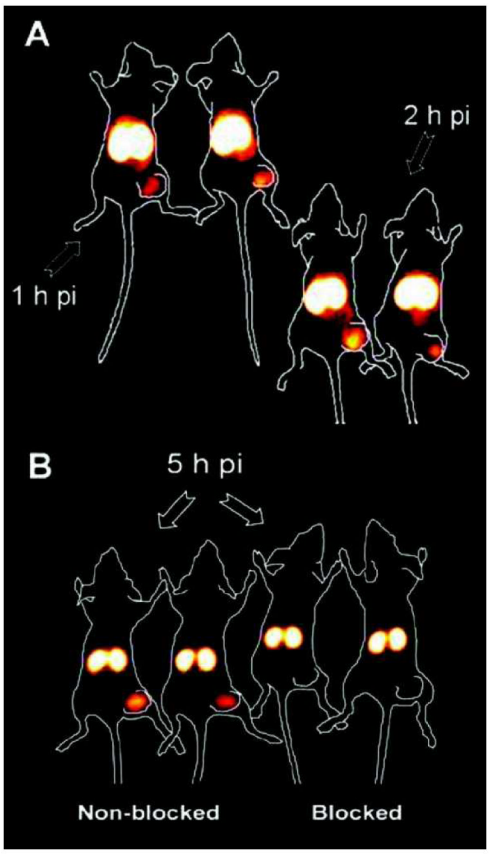


**Fig. (1).**
Radioimmunoscintigraphy (RIS) of HER-2-positive SKOV-3 tumor-bearing mice with $^{99m}$Tc-labeled $Z_{HER-2:342}$ affibody. (A) At 1 h and 2 h post-injection (pi), tumors were visualized on the right hind legs. (B) A better image contrast was obtained at 5 h pi. As a negative control, a pre-injected dose of excess unlabeled affibody blocked tracer uptake in the tumor. Adapted from [55].

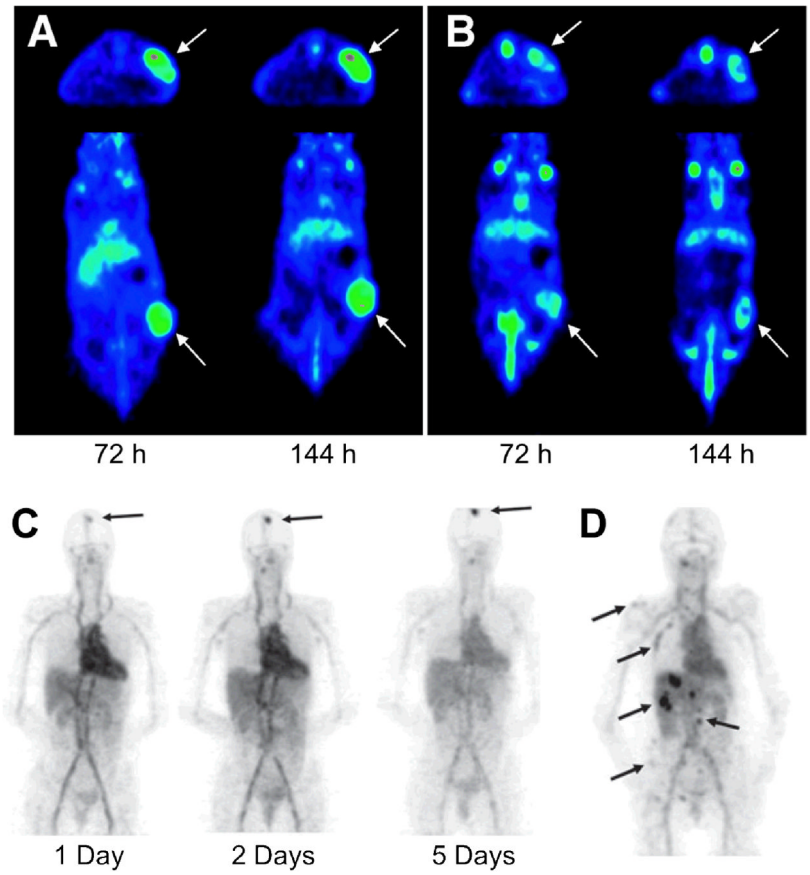


**Fig. (2).**

PET imaging of HER-2 expression with $^{89}$Zr-trastuzumab. Serial transverse and coronal PET images of a mouse administered with $^{89}$Zr-trastuzumab before (A) and after (B) three dosages of anticancer drug (HSP90 inhibitor) NVP-AUY922 are shown here. Arrows indicate the HER-2 positive tumors. (C) $^{89}$Zr-trastuzumab PET scans of a patient already on trastuzumab treatment at different time points post-injection revealed an increase over time of the tumor-to-nontumor ratio of tracer uptake. Arrow indicates $^{89}$Zr_trastuzumab uptake in the only lesion. (D) $^{89}$Zr-trastuzumab PET of a patient with liver and bone metastases at 5 days post-injection. A number of lesions are indicated by arrows. Adapted from [73, 80].

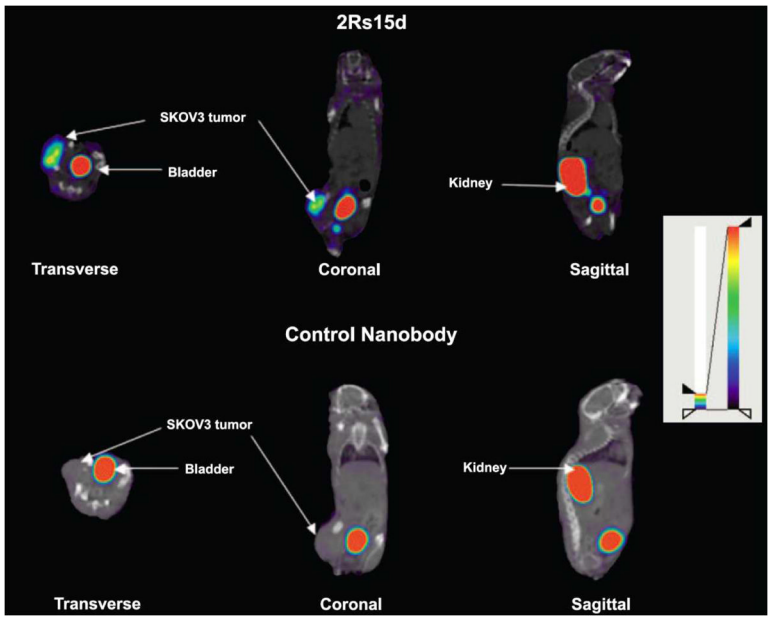


**Fig. (3).**

Fused SPECT/CT images (transverse, coronal and sagittal views) of mice with HER-2 positive SKOV3 tumor. Images were obtained at 1 h after injection of $^{99m}$Tc-labeled HER-2 targeting nanobody (2Rs15d) or a control nanobody. Adapted from [90].

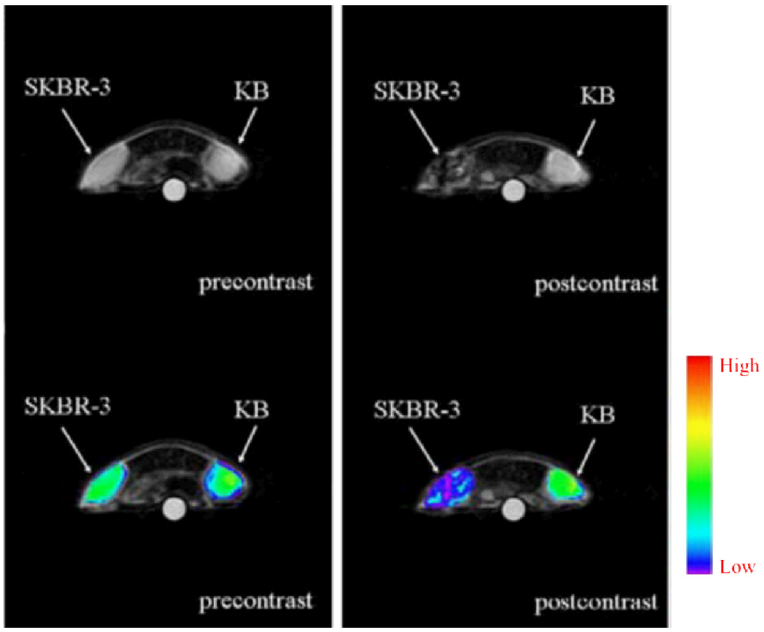


**Fig. (4).**

$T_2$-weighted MRI images (Top: grayscale; Bottom: color-map) of tumor-bearing mice before and at 1 h after injection of trastuzumab-conjugated nanoparticles. The mice were implanted with both HER-2 positive SKBR-3 and HER-2 negative KB tumors. Adapted from [105].

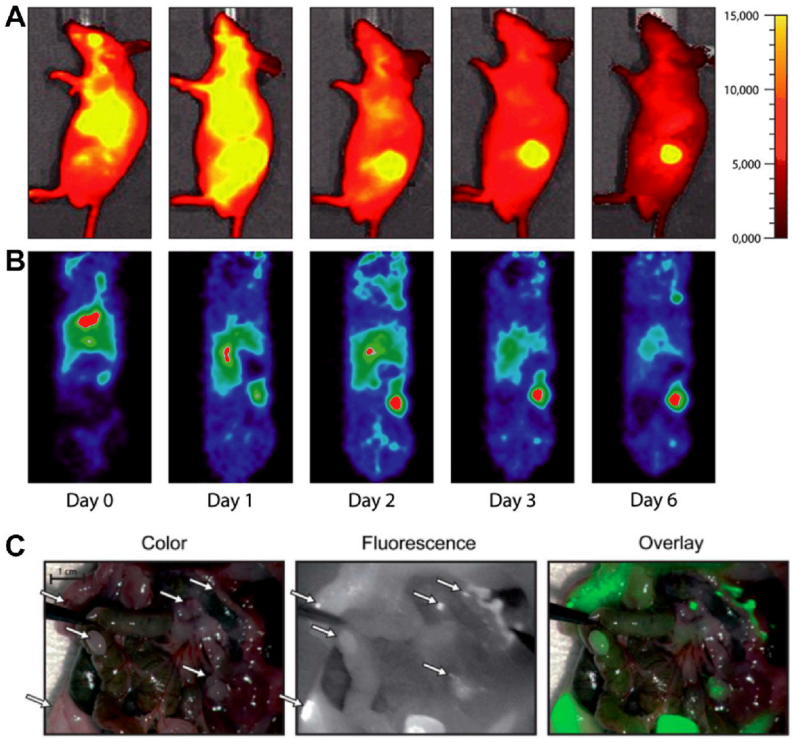


**Fig. (5).**

Dualmodality imaging of HER-2 in subcutaneous SKBR-3 tumor-bearing mice. (A) NIRF imaging with IRDye800CW-labeled trastuzumab (sagittal view). (B) PET imaging with $^{89}$Zr-trastuzumab (coronal view). (C) Images of mouse bearing human gastric cancer KATO-III intraperitoneal tumor captured by intraoperative camera. IRDye800CW-labeled trastuzumab was administered to mice on a diet that minimizes autofluorescence in the peritoneum. NIRF imaging was taken on day 4 after injection. White arrows indicate the tumors, which were also shown in green in the overlay of color picture and a NIRF image. Adapted from [124].

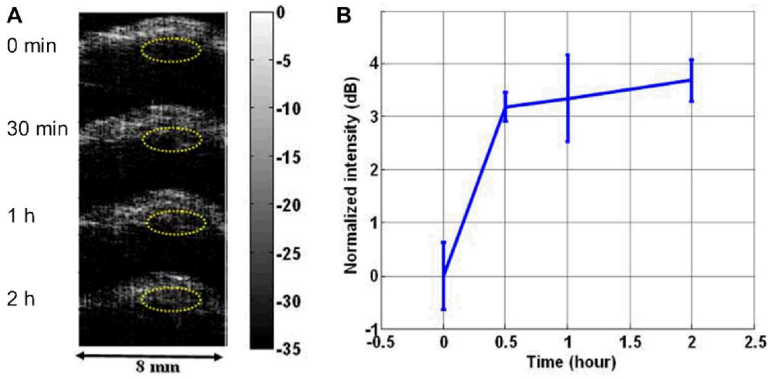


**Fig. (6).**

(A) *In vivo* photoacoustic images of OECM1 tumor before and after injection of trastuzumab-conjugated gold nanorods. Eclipsed dashed circles indicate the tumor regions. (B) The time-dependent image signal intensity of the tumor region. Adapted from [147].

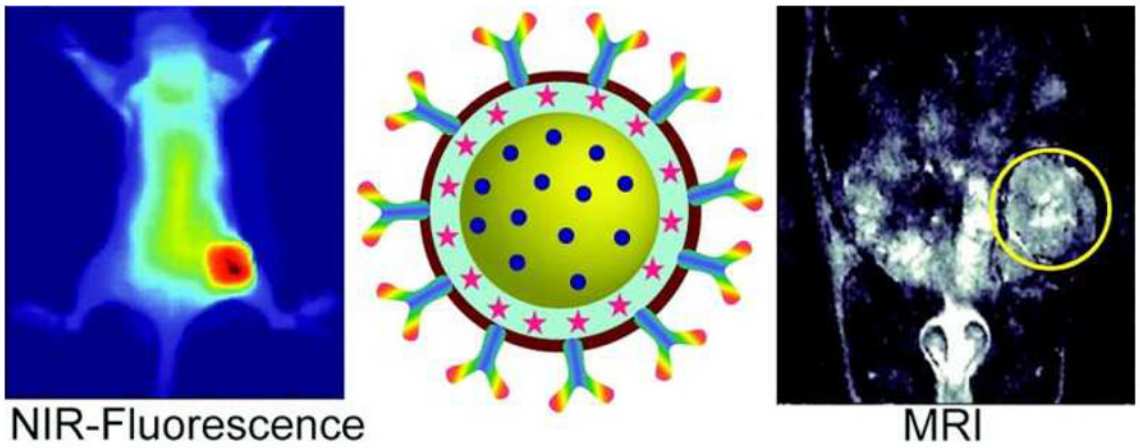


**Fig. (7).**
Tracking of multimodal therapeutic nanocomplexes targeting breast cancer *in vivo* with both NIRF imaging and MRI. Adapted from [155].

## Table 1

Current clinical studies of antibody-based imaging of HER-2 (Information based on www.clinicaltrials.gov).

| Clinical Trial Number | Radiolabeled antibody | Imaging technique | Treatment | Status |
|---|---|---|---|---|
| NCT01445054 | $^{111}$In-Trastuzumab | RIS | | Phase I |
| NCT00605397 | $^{64}$Cu-Trastuzumab | PET | | Pilot Trial |
| NCT00613847 | $^{68}$Ga-F(ab′)2-Trastuzumab | PET | | |
| NCT01081600 | $^{89}$Zr-Trastuzumab | PET | AUY922 | Phase I/II |
| NCT01420146 | $^{89}$Zr-Trastuzumab | PET/CT | | Phase I |
| NCT01565200 | $^{89}$Zr-Trastuzumab | PET/CT | T-DM1 | Phase II |
| NCT01216033 | $^{111}$In-ABY-025 | SPECT | | Phase I/II |
| NCT00474578 | $^{111}$In-Trastuzumab | RIS/SPECT | | Phase I |